Earth and Planetary Science Letters 492 (2018) 232–238

Contents lists available at ScienceDirect

Earth and Planetary Science Letters

www.elsevier.com/locate/epsl

A low-angle detachment fault revealed: Three-dimensional images of the S-reflector fault zone along the Galicia passive margin

C. Nur Schuba [a], Gary G. Gray [a], Julia K. Morgan [a], Dale S. Sawyer [a], Donna J. Shillington [b], Tim J. Reston [c], Jonathan M. Bull [d], Brian E. Jordan [a,e]

[a] Department of Earth, Environmental and Planetary Sciences, Rice University, MS-126 Main Street, 77005, Houston, TX, USA
[b] Lamont-Doherty Earth Observatory, Columbia University, 61 Route 9W, PO Box 1000, 10964-8000, Palisades, NY, USA
[c] School of Geography, Earth and Environmental Sciences, University of Birmingham, Edgbaston, Birmingham, B15 2TT, UK
[d] National Oceanography Centre Southampton, University of Southampton, Southampton, S014 3ZH, United Kingdom
[e] BP America Inc., 501 WestLake Park Blvd., 23.126C, 77079, Houston, TX, USA

ARTICLE INFO

Article history:
Received 19 December 2017
Received in revised form 2 April 2018
Accepted 8 April 2018
Available online xxxx
Editor: J.-P. Avouac

Keywords:
rifting
detachment faults
Galicia margin
continent–ocean transition zone
fault rock production
fault surface morphology

ABSTRACT

A new 3-D seismic reflection volume over the Galicia margin continent–ocean transition zone provides an unprecedented view of the prominent S-reflector detachment fault that underlies the outer part of the margin. This volume images the fault's structure from breakaway to termination. The filtered time-structure map of the S-reflector shows coherent corrugations parallel to the expected paleo-extension directions with an average azimuth of 107°. These corrugations maintain their orientations, wavelengths and amplitudes where overlying faults sole into the S-reflector, suggesting that the parts of the detachment fault containing multiple crustal blocks may have slipped as discrete units during its late stages. Another interface above the S-reflector, here named *S′*, is identified and interpreted as the upper boundary of the fault zone associated with the detachment fault. This layer, named the S-interval, thickens by tens of meters from SE to NW in the direction of transport. Localized thick accumulations also occur near overlying fault intersections, suggesting either non-uniform fault rock production, or redistribution of fault rock during slip. These observations have important implications for understanding how detachment faults form and evolve over time. 3-D seismic reflection imaging has enabled unique insights into fault slip history, fault rock production and redistribution.

1. Introduction

Detachment faults are major structures in many extensional settings, accommodating many kilometers of displacement, particularly in regions of extreme crustal thinning (i.e. rift zones and continent–ocean transitions) (e.g. Davis and Lister, 1988; Escartín et al., 2008; John and Cheadle, 2010). Despite their importance, our knowledge of such large-displacement faults is incomplete. 2-D seismic profiles over passive margins (Lister et al., 1991; Reston, 2007; Osmundsen and Ebbing, 2009) and active rift zones (Flotté et al., 2005; Goodliffe and Taylor, 2007) confirm that these faults are widespread features characterized by pronounced reflections denoting significant property contrasts, but offer little insight into the internal structures and properties of such faults. Limited surface exposures and outcrops, in both subaerial and submarine settings, provide local windows into these faults (e.g. John, 1987; Cann et al., 1997; Florineth and Froitzheim, 1994; Manatschal and Nievergelt, 1997; Manatschal, 1999), revealing fault zone structure and morphology, but typically provide poor constraints on fault extents or spatial variability. In the absence of more comprehensive views of detachment faults and their variations, we are challenged to understand the full role that detachment faults play during crustal extension.

A new 3-D seismic reflection volume was collected in 2013 over the Galicia margin (Fig. 1), with the goal of imaging the structure of the continent–ocean transition zone. This area is underlain by the prominent S-reflector detachment fault (Reston, 1996). This new seismic volume has improved resolution compared to older 2-D data. It also covers the S-reflector detachment fault in full 3-D over a ~600 km^2 area. Thus, for the first time ever, we have the opportunity to peer into an extensive detachment fault to examine its first order 3-D structure, as well as variations in its characteristics, from breakaway to termination. These unique observations enable us to assess deformation processes, fault properties and evolution, with implications for extensional processes in similar settings around the world.

E-mail address: nur.schuba@rice.edu (C.N. Schuba).

https://doi.org/10.1016/j.epsl.2018.04.012

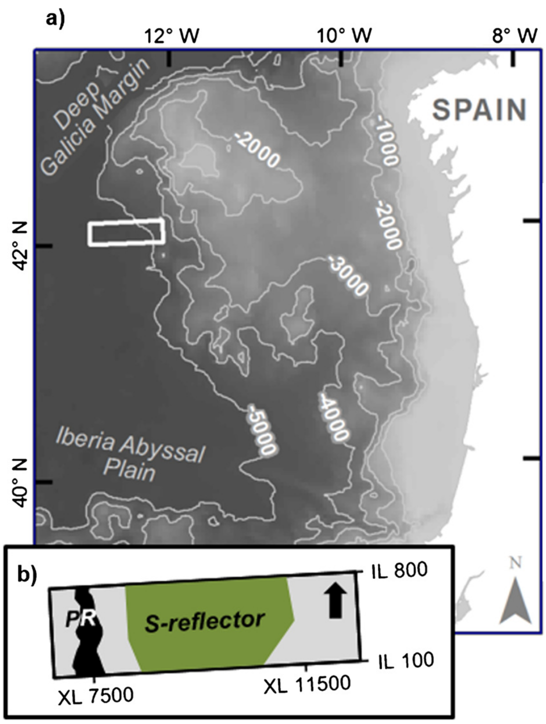

Fig. 1. a) Survey location over Galicia margin located west of Spain. White box shows the location of 3-D seismic reflection survey. b) Enlarged view of survey area, showing 600 km^2 areal extent of S-reflector within seismic volume. *PR: peridotite ridge, IL: inline, XL: crossline*.

2. Geologic setting and the S-reflector

The Deep Galicia passive margin was generated by amagmatic rifting and break-up between southern Europe and North America in three phases between Late Triassic to Aptian time (Boillot et al., 1989; Péron-Pinvidic et al., 2013; Tucholke et al., 2007). Rift-related structures are well preserved and readily imaged within this relatively sediment-starved margin (Reston et al., 1996; Dean et al., 2000; Whitmarsh et al., 1990; Borgmeyer, 2010). The majority of the late stage crustal thinning was accommodated by slip along the regional low-angle S-reflector detachment fault (Reston et al., 1996), which can be mapped over an area of ~2100 km^2 on 2-D seismic lines that span the margin (Borgmeyer, 2010). The S-reflector cuts through continental crust to the east, and places upper continental crust over serpentinized upper mantle to the west (Boillot et al., 1989; Reston, 1996; Reston et al., 1996; Bayrakci et al., 2016). The continental crustal blocks overlying the S-reflector show similarities to the rider blocks observed by Reston and Ranero (2011) and modeled by Choi et al. (2013).

The seismic character of the S-reflector has been constrained by waveform and trace analyses of 2-D reflection data (Reston, 1996; Leythaeuser et al., 2005). The continuous high reflection amplitude, positive polarity reflector denotes a sharp step increase in impedance, consistent with continental crust over serpentinized peridotite, further supporting the detachment fault interpretation (Reston, 1996). Leythaeuser et al. (2005) used 1-D full waveform inversion to tentatively identify a ~50-m-thick low-velocity zone immediately overlying the S-reflector. They interpreted this zone to represent serpentinized peridotite derived from the footwall and/or intensely damaged and brecciated hanging wall rocks.

The new seismic volume permits examination of this fault zone in 3-D and at higher resolution to ascertain if the characteristics noted above hold true over its entire extent, and what might account for any variations. In addition, the 3-D imaging provides a rare view into the 3-D morphology of a detachment fault zone over an extremely large area, something that has never been seen before.

3. Seismic data and results

The study area and footprint of the seismic survey are shown in Fig. 1. The prestack time-migrated and noise-reduced 3-D seismic volume is 68 km wide (E-W) and 20 km long (N-S) with a 13 second record window. The data were collected using four 6-km streamers with a receiver spacing of 12.5 m. The acquisition azimuth was 87°. The polarity of the data is American-standard (a downward increase in acoustic impedance is displayed as a peak). Additional information about data acquisition and processing can be found in the supplementary information.

A representative section through the 3-D seismic volume is shown in Fig. 2a. The S-reflector stands out prominently from its eastern breakaway that cuts through continental crust to where it abruptly loses reflection amplitude beneath a broad basin to the west. Rotated fault blocks above the S-reflector record crustal thinning accommodated by slip along the S-reflector. The S-reflector was interpreted in the time domain along the peak reflection amplitude of the deepest continuous high amplitude positive polarity reflection (Fig. 2b). This is consistent with other workers (de Charpal et al., 1978; Boillot et al., 1989; Reston et al., 1996; Leythaeuser et al., 2005; Borgmeyer, 2010). All interpretations were carried out with the Schlumberger software Petrel^{TM} on every fifth inline and crossline. The resulting grids of horizon interpretation were then interpolated into continuous surfaces.

The time structure map of the resulting *S* fault surface reveals two distinct characteristics (Fig. 3a). Broad NNE/SSW oriented highs and lows correlate with the presence of rotated continental blocks that overlie the detachment fault. These high velocity crystalline rocks create velocity pull-up beneath them, in contrast to the lower velocity sedimentary units that lie in between the crustal blocks. These time-structure highs, therefore, are generally located between intersections with the overlying faults. In addition, smaller scale undulations, generally oriented NW-SE, are also present across the entire extent of the *S* fault surface. Their trends differ noticeably from the acquisition azimuth of 87°, confirming that they are not simply acquisition artifacts.

A spatial bandpass filter was applied to the surface to visually enhance the prominent NW-SE undulations on the S-reflector. This filter, with lower and higher limits of 80 m and 500 m, was used to remove both large wavelength fluctuations due to the velocity pull-up effect, and high frequency noise. The resulting map (Figs. 3b, S1) reveals the prominent NW-SE undulations, as linear corrugations in the S-reflector time structure. These corrugations are present across the entire *S* surface. The trends of the corrugations vary from 95° in the south, to 115° in the northwest, with an average azimuth of 107°. The crest-to-crest wavelengths of these corrugations range between 200–600 m, and their crestal lengths are 3–7 km. Interestingly, many of the corrugations appear to be co-linear and/or continuous across mapped fault intersections (Fig. 3b). The peak-to-trough heights of the corrugations are within the limits of detectability without being fully resolved (Sheriff, 1985; Simm and Bacon, 2004). They range from 10 to 20 ms, which correspond to ~25–50 m using the velocity determined by Leythaeuser et al. (2005).

A second interface associated with the S-reflector is also recognizable across the 3-D volume. This surface, here named S', occurs as a more or less continuous negative polarity reflection above the S-reflector. The S' reflection is seismically less coherent than S, because the absolute reflection amplitude is more variable and can be as little as one third of the S reflection amplitudes (Fig. 2b). The S and S' surfaces while roughly conformable, are not parallel, with notable divergence in certain areas. The S-reflector seismic